J. Biochem. **141,** 279–286 (2007)
doi:10.1093/jb/mvm038

Mutational Analysis of the Carboxyl-terminal Region of the SV40 Major Capsid Protein VP1

Naoki Yokoyama[1], Masa-aki Kawano[1], Hiroko Tsukamoto[1], Teruya Enomoto[1], Takamasa Inoue[1], Ryou-u Takahashi[1], Akira Nakanishi[2], Takeshi Imai[2], Tadashi Wada[1,3] and Hiroshi Handa[1,*]

[1]Graduate School of Bioscience and Biotechnology, and [3]Integrated Research Institute, Tokyo Institute of Technology, 4259 Nagatsuta, Midori-ku, Yokohama 226-8503, Japan; and [2]National Institute of Longevity Sciences, 36-3 Gengo, Morioka-machi, Obu 474-8511, Japan

Received November 21, 2006; accepted December 10, 2006; published online February 5, 2007

Virus-like particles (VLPs), a promising next-generation drug delivery vehicle, can be formed *in vitro* using a recombinant viral capsid protein VP1 from SV40. Seventy-two VP1 pentamers interconnect to form the *T* = 7*d* lattice of SV40 capsids, through three types of C-terminal interactions, α-α′-α″, β-β′ and γ-γ. These appear to require VP1 conformational switch, which involve in particular the region from amino acids 301–312 (herein *Region I*). Here we show that progressive deletions from the C-terminus of VP1, up to 34 amino acids, cause size and shape variations in the resulting VLPs, including tubular formation, whereas deletions beyond 34 amino acids simply blocked VP1 self-assembly. Mutants carrying in *Region I* point mutations predicted to disrupt α-α′-α″-type and/or β-β′-type interactions formed small VLPs resembling *T* = 1 symmetry. Chimeric VP1, in which *Region I* of SV40 VP1 was substituted with the homologous region from VP1 of other polyomaviruses, assembled only into small VLPs. Together, our results show the importance of the integrity of VP1 C-terminal region and the specific amino acid sequences within *Region I* in the assembly of normal VLPs. By understanding how to alter VLP sizes and shapes contributes to the development of drug delivery systems using VLPs.

Key words: baculovirus, carboxyl-terminal of VP1, self-assembly, simian virus 40, virus-like particles.

INTRODUCTION

Simian Virus 40 (SV40) is a non-enveloped small DNA tumour virus belonging to the papovavirus family. Its ~50 nm diameter capsid consists of 72 pentamers of the major capsid protein, VP1, enclosing ~72 molecules of the minor capsid proteins, VP2 and VP3, as well as the viral genome. The structure of the capsid has been resolved by X-ray crystallography, and shows that the VP1 pentamers are arranged in a *T* = 7*d* lattice (*1*, 2). Each VP1 pentamer is linked via the C-terminal arm of VP1, which extends to and interdigitates with the amino (N)-terminal region of a molecule of VP1 in a neighbouring pentamer. C-terminal arms of adjacent pentamers also contact each other. Such C-terminal–C-terminal interactions involve a distinct structural switch region of the VP1 C-terminus, between amino acids 301 and 312 [VP1(301–312)]. Six distinct conformations of VP1 have been observed in the virion (α-α′-α″, β-β′ and γ), with the most variable region of the protein being VP1(301–312) (*1*, 2). As such, the structural switch region VP1(301–312) may be particularly relevant to the proper positioning of the VP1 pentamer and the arrangement of the icosahedral pentamer lattice.

Biochemical analysis has shown that SV40 VP1-mutants lacking the C-terminal 58 residues formed pentamers, but did not assemble into particles, consistent with a structural model in which the C-terminal arm is the only connection between pentamers (*3*). Several point mutants of the C-terminal region of VP1 do not assemble into an icosahedral capsid with a *T* = 7*d* lattice, but rather, formed deformed, or tubular capsids, or a sheet unable to properly close and form a particle (*4*). Thus, it appears that the C-terminal region is essential for proper self-assembly of VP1 pentamers. However, functional dissection of the role of the C-terminal region of VP1 on pentamer assembly has yet to be carried out.

In many polyomaviruses, including SV40 (*5*, 6), JC virus (*7*, 8), BK virus (BKV) (*9*, 10), mouse polyomavirus (*11*, 12) and avian polyomavirus (*13*, 14), the ability of VP1 to assemble into a spherical capsid under various conditions has been examined both *in vivo* and *in vitro*. Recombinant VP1 produced in non-permissive mammalian cells, insect cells and *Escherichia coli* can form virus-like particles (VLPs) without the internal viral components VP2, VP3 and minichromosomal viral DNA (*15*). Purified VP1 pentamers of mouse polyomavirus can assemble into VLPs, as well as polymorphic assemblies, in a defined chemical solution (*16*). We have shown that SV40–VLP assembly occurs effectively in insect cells using a baculoviral expression system (*17*). Using this system, we showed that neither cysteine

*To whom correspondence should be addressed. Tel: +81-45-924-5872, Fax: +81-45-924-5834, E-mail: hhanda@bio.titech.ac.jp

residues, including Cys 104, nor Ca-binding sites are essential for SV40 VP1 assembly, consistent with *in vivo* analyses of these residues (*5*).

Here we have focussed on the role of the VP1 C-terminal arm on capsid assembly, and sought to define the essential region for VP1 self-assembly using a baculoviral expression system. Our results suggest that elements in the region of VP1 between amino acids 301 and 361 are collectively important for VP1 assembly. However, detailed analysis on the first region, VP1 (301–312), revealed that the region is important for assembly of a full capsid of $T=7d$ symmetry: point mutations aiming to disrupt the structural switch region of VP1(301–312) led to blockade of full-capsid formation, but allowed to form small particles resembles those that had $T=1$ icosahedral symmetry. Our results indicate that in the VP1 C-terminal region, VP1(301–312) is important for the structural switch of the inter-pentamer links, and is thereby guiding the self-assembly process of the pentamer to form a full capsid with a $T=7d$ lattice.

METHODS

Plasmid Construction of VP1 Mutant—A baculoviral expression plasmid, pFastBac1-VP1, was constructed as follows. PCR was used to amplify DNA fragments encoding VP1 with a *Sal*I restriction site introduced into the 5′ end, using SV40 genomic DNA as a template. The fragments were end-filled by Blunting high kit (Takara), then digested with *Sal*I. The vector pBluscriptII SK+ was digested with ApaI, end-filled using Blunting high kit, digested with SalI, and ligated with the VP1 PCR fragment to generate pBS-VP1. A SalI-KpnI fragment of VP1 generated from pBS-VP1 was inserted into pFastBac1 digested with SalI-KpnI to generate pFastBac1-VP1.

All VP1 deletion mutants and point mutants were introduced into pFastBac1-VP1. Sequences of primers and linkers used for PCR and construction of the VP1 variants will be provided upon request. All mutants were confirmed by dideoxy nucleotide sequence analysis.

Bacmid clones harbouring baculoviral DNA containing a VP1 expression cassette were generated by transforming the various pFastBac-VP1 plasmids into DH10Bac *E. coli* utilizing the Bac-to-Bac baculovirus expression system (Invitrogen). Bacmids were purified prior to transfection into insect cells.

Expression and Purification of VP1 in Sf9 Cells—Expression of SV40 VP1 mutants in *Spodoptera frugiperda* (Sf-9) cells was previously described (*5*, 17–19). Briefly, 3×10^7 cells were infected with baculovirus expressing recombinant VP1 proteins at a multiplicity of infection of 5 to 10. Cells were collected 72 h post-infection by scraping, resuspended in 20 mM Tris–HCl (pH 7.9) containing 0.1% sodium deoxycholate and protease inhibitor cocktail, sonicated, then centrifuged at $15{,}000\times g$ for 10 min at 4°C. The supernatant (100 μl) was loaded onto a 20–50% cesium density gradient (5 ml) containing 20 mM Tris–HCl (pH 7.9), then centrifuged at $237{,}000\times g$ for 3 h at 4°C in an SW55Ti rotor (Beckman). After centrifugation, samples were collected from the top of the gradient and subjected to SDS-polyacrylamide gel electrophoresis (SDS-PAGE). Proteins were visualized using Coomassie brilliant blue. VP1 peak fractions were selected for observation by electron microscopy.

Electron Microscopy—Examination of VP1 mutants by electron microscopy has been described previously (*5*, 17–19). Briefly, 5 μl of VP1 peak fractions collected from cesium density gradients were mounted on glow-discharged carbon-coated copper grids (Nisshin EM); excess material was removed by touching with filter paper. The grid was washed with water, briefly placed onto a droplet of 2% uranyl-acetate solution, air dried, and stored in a desiccated environment. The samples were viewed using a Hitachi 7500 electron microscope, operating at 100 kV at an apparent magnification of 25,000–50,000.

Sucrose Sedimentation Analysis—Sucrose sedimentation analysis of Sf-9 cell lysates expressing recombinant VP1 mutants has been previously described (*5*, 17, 19). Briefly, cell lysate (20 μl) was loaded onto 0.6 ml of a preformed 20–40% sucrose gradient containing 20 mM Tris–HCl (pH 7.9) with appropriate adapters, then centrifuged at $286{,}800\times g$ for 1 h at 4°C in a SW55Ti rotor. Fractions (55 μl) were collected from the top of the gradient, and an aliquot of each fraction (7 μl) was separated by SDS-PAGE, then analysed by immunoblot using anti-SV40 polyclonal antibody (courtesy of M. Ikeda and I. Tamai, MBL, Nagoya, Japan). Immuno-reactive bands were visualized using the enhanced chemiluminescence system (GE Healthcare).

RESULTS AND DISCUSSION

C-terminal Region of VP1—Based on the existing structural model (*1*, 2), we tentatively divided the C-terminal region of SV40 VP1 into four regions, *Regions I–IV* (Fig. 1a and c). *Region I* (amino acids 301–312) forms an amphipathic α-helix (Fig. 1a, c and d, coloured in red) and engages non-equivalent interactions between α-helices at inter-pentameric contacts (α-α′-α″, Fig. 1b, top panel; and β-β′, Fig. 1b, middle panel). However, *Region I* does not assume an amphipathic α-helix structure where γ-γ interactions occur between pentamers (Fig. 1b, bottom panel). *Region II* (amino acids 313–329, Fig. 1a, c and d, coloured in green) and *Region III* (amino acids 330–344) contain β-strands (Fig. 1a, c and d, coloured in yellow), and make identical contacts with the interacting VP1 in all VP1 conformations. *Region II* forms hydrogen bonds with N-terminal residues of the VP1 of a neighbouring pentamer, including Glu-48, Phe-50, Asp-198 and Asp-200. Amino acids 320–327 in *Region II*, VP1(320–327), adopt a loop structure that has been implicated in the association of the N-terminal region of VP1 with neighbouring pentamers. *Region III* (Fig. 1a, c and d, coloured in yellow) is stacked with hydrogen bonds of two N-terminal β-strands of interacting VP1, VP1(21–30) and VP1(44–55). *Region IV* (amino acids 345–361, Fig. 1a, c and d, coloured in purple) is highly mobile and forms either a β-sheet by itself, or a loop, both of which make

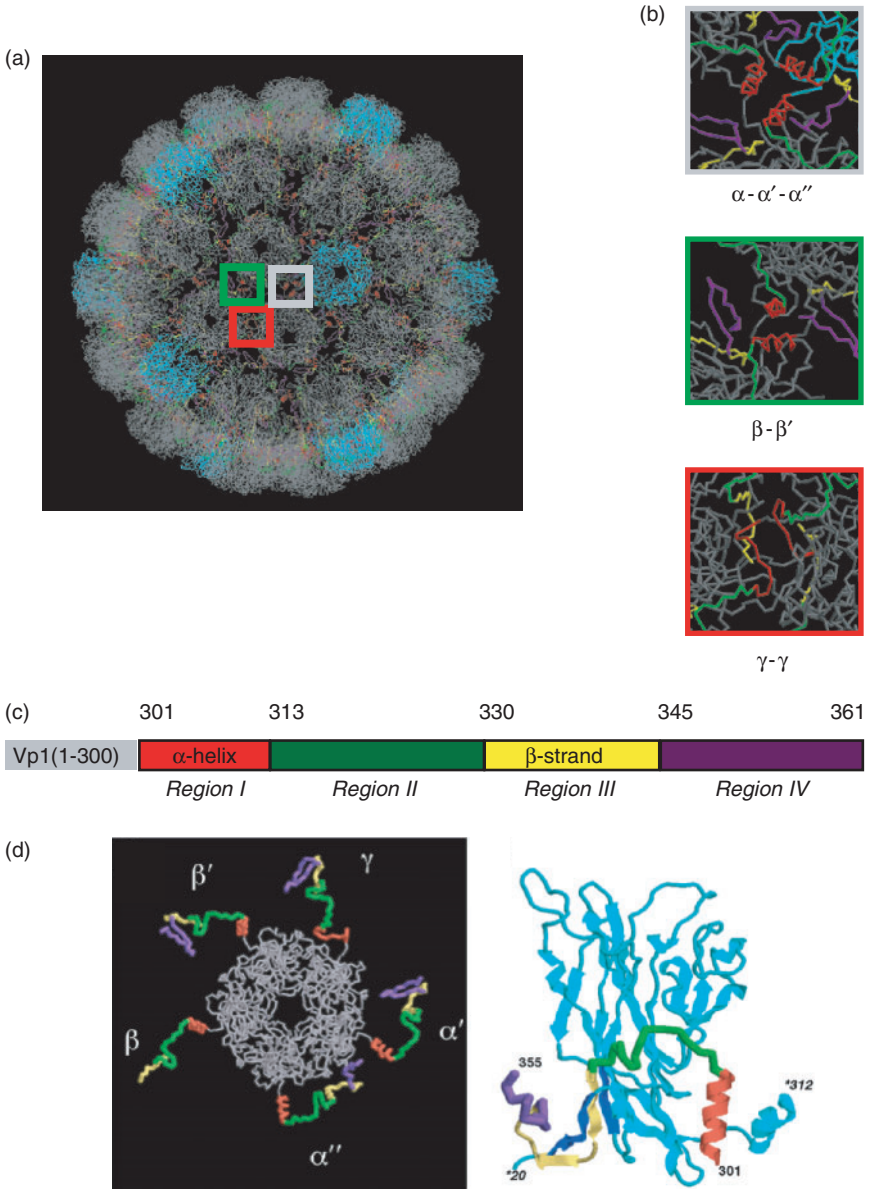

Fig. 1. **Structures of the carboxyl-terminal regions in the VP1 pentamer.** (**a**) C-α backbone drawing of SV40 virions reconstructed from the structural unit of the SV40 VP1 capsid [1SVA (*2*)] using VIPER (*22*). Pentavalent VP1 pentamers (VP1 pentamers surrounded by five pentamers) are marked in light blue. The C-terminal arm regions, VP1(301–312), (313–329), (330–344) and (345–361), are coloured in red, green, yellow and purple, respectively. The positions of three distinct interaction-types of the C-terminal arm in the SV40 particle are shown in the gray square (α-α′-α″), green square (β-β′) and red square (γ-γ). (**b**) Close-up views of structures of the three types of interaction of the C-terminus are shown in the white square (α-α′-α″), green square (β-β′), and red square (γ-γ). (**c**) Schematic representation of the SV40 VP1 C-terminus; the VP1 C-terminal regions, structurally categorized according to Stehle *et al*. (*2*), are coloured as in (**a**). (**d**, left panel) backbone drawing of a VP1 pentamer showing α′, α″, β, β′, and γ conformations. VP1 C-terminal arms are colored as in (**a**). (**d**, right panel) side-view of the VP1 monomer with an invading C-terminal arm from the neighbouring pentamer; VP1 monomer, coloured in cyan, and the invading C-terminal arm, coloured as in (**a**), are shown in ribbon drawing. The N-terminal of VP1, VP1(22–30) and VP1(44–48), is coloured in blue. The first and the last residues of the VP1 monomer (italicized with asterisk) and the C-terminal arm (standard) are marked. Amino acid residues are numbered as in Liddington *et al*. (*1*).

several contacts with the facing VP1 of the adjacent pentamer.

The C-terminal Region of VP1 is Important for VLP Formation—In order to determine the regions important for assembly of VP1-pentamer and forming a full capsid, we constructed a series of C-terminal deletion mutants, and expressed them in Sf9 cells using baculoviral vectors (Fig. 2a). Sf-9 lysates containing VP1 mutant proteins were subjected to 20–50% cesium chloride density gradient centrifugation, and fractions were separated by SDS-PAGE, followed by staining with Coomassie brilliant blue (data not shown). Fractions containing

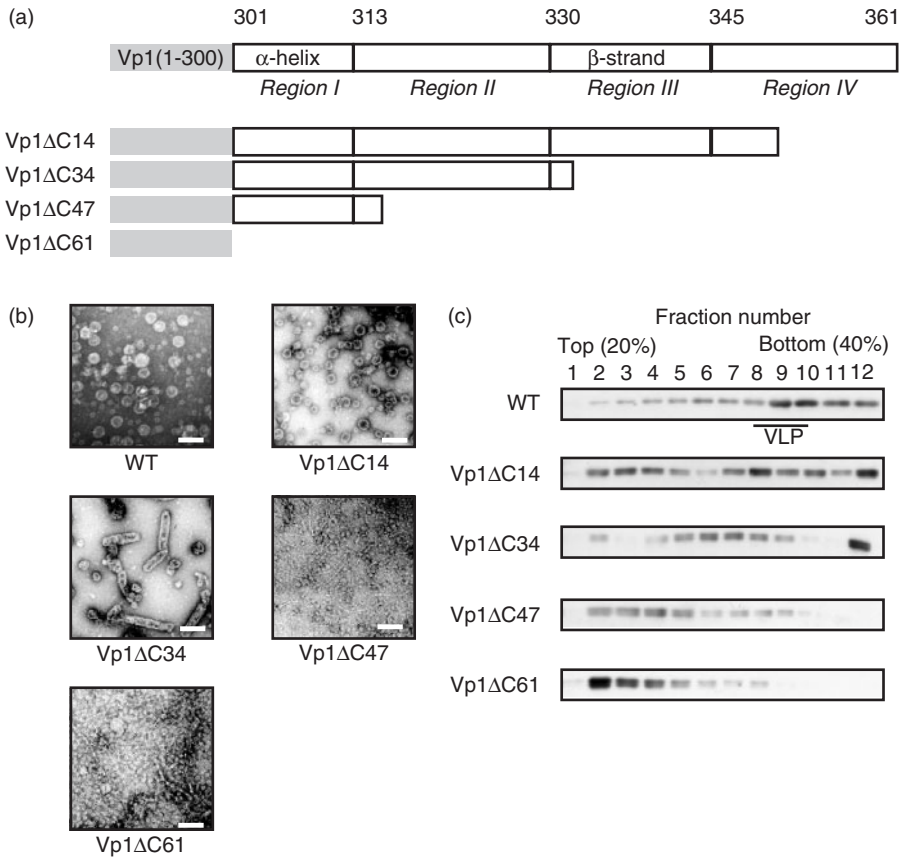

Fig. 2. **Assembly of VP1 deletion mutants expressed in Sf-9 cells.** (**a**) Schematic representation of VP1 C-terminal deletion mutants. (**b**) Electron micrographs of VP1 deletion mutants after purification by CsCl density gradient centrifugation. Fraction containing most abundant VP1 was used to visualize VP1 assemblies by uranyl acetate negative staining. Scale bars indicate 100 nm in WT, VP1ΔC14 and VP1ΔC34, and 50 nm in VP1ΔC47 and VP1ΔC61. (**c**) Sucrose gradient sedimentation analysis. Cell lysates containing the indicated VP1 deletion mutants were fractionated by 20–40% sucrose gradient sedimentation. Aliquots of each fraction from the top to the bottom of the gradient were subjected to SDS-PAGE and Western blot analysis using anti-VP1 antibody.

the largest amount of the 45 kDa protein corresponding VP1 were examined using electron microscopy (EM) (Fig. 2b). Wild-type VP1 assembled into two types of particles: majority of VP1 formed large VLPs 40–45 nm in diameter, and some VP1 assembled to small spherical particles ~20 nm in diameter (Fig. 2b, WT). Mutants lacking the C-terminal 14 amino acids (aa) of VP1, which comprise most of *Region IV*, VP1ΔC14, formed spherical particles, but their diameters varied significantly, ranging from 20 to 50 nm. Many VP1 pentamers were also detected (Fig. 2b, VP1ΔC14). Mutants lacking the C-terminal 34 aa, and lacking *Region III* and *IV*, VP1ΔC34, formed non-spherical, aberrant assemblies, as well as tubules (Fig. 2b, VP1ΔC34). Two deletion mutants, VP1ΔC47 and VP1ΔC61, containing one (*Region I*) and none of the C-terminal regions, respectively, did not form any assemblies, and remained as VP1 pentamers (Fig. 2b, VP1ΔC47, VP1ΔC61).

To confirm the earlier results, sucrose sedimentation analysis of Sf-9 cell lysates containing wild-type VP1 and the deletion mutants was performed (Fig. 2c). Wild-type VP1 was detected in fractions 8–10, corresponding to VLP peak fractions (Fig. 2c, WT). Free VP1 pentamers were also detected in the upper fractions of the gradient. VP1ΔC14 was distributed through out the gradient, (Fig. 2c, VP1ΔC14), consistent with EM observations that VP1ΔC14 formed particles of various sizes, from 20 to 50 nm in diameter. The presence of free pentamer suggested that VP1ΔC14 particles may dissociate into pentamers during preparation, implying that the particles are unstable. Thus, *Region IV* could play a role in sustaining the stability of VP1 particles. VP1ΔC34 mutants were apparently defective in forming spherical particles, and EM analysis showed that these mutant VP1 proteins assembled into aberrant structures or tubules. In the sucrose sedimentation assay, VP1ΔC34 mutants were distributed in fractions 4–9, as well as in the bottom fraction indicating that majority of VP1 did not assemble to VLPs rather forming aberrant structures, consistent with the idea that the C-terminal 34 residues encompassing *Regions III* and *IV*, are important for proper VP1 assembly. Sedimentation analysis of VP1ΔC47 and VP1ΔC61 revealed that both of these mutant VP1 proteins were distributed predominantly in the upper fractions, indicating that they failed to self-assemble (Fig. 2c, VP1ΔC47, VP1ΔC61).

These results suggested that at least *Region II* is important for the inter-pentamer interaction and VP1 self-assembly. However, implication of *Region I*'s role could not be ruled out. *Region II* contacts with N-terminal residues of interacting VP1, which likely to hold ability to tie two VP1 pentamer together, but seemed not sufficient for forming ordered spherical particles. *Region III* is the integrate part of inter-pentamer bonding and the results obtained here are consistent with the structural model that, in together with *Region IV*, it is important for proper inter-pentameric interactions for achieving formation of a full capsid. Thus, the C-terminal regions appeared to hold multiple functions on VP1 assembly to capsid, indicating that the C-terminal regions are collectively important for VP1–VLP formation. The limit of deletional analysis here is that it is difficult to analyse the function of individual region. We next focused on the role of each individual region, with emphasis on *Region I*, VP1(301–312) using point-mutational approach.

Mutational Analysis of Region I of the VP1 C-terminal Region—Region I forms an α-helix that participates in two types of inter-pentameric interactions, α-α′-α″-type and β-β′-type. We constructed two mutants, L305P and L308P, in which one of two highly conserved leucine residues was altered to proline. From the structural model, these two leucines are positioned in the core of the hydrophobic contact between the α-helices, and substitution to proline would disrupt the α-helix and the hydrophobic contact (Fig. 3a). Sucrose gradient sedimentation analysis revealed that L305P and L308P mutants were present in fractions 2–5 (Fig. 3b, L305P, L308P), indicating that these two mutants failed to form VLPs. Close examination by EM of the VP1 peak fraction of CsCl density gradient centrifugation showed that some VP1 of these two mutant proteins formed protein aggregates, consistent with the results of sucrose gradient analysis indicating that they were defective in forming a full VLP (Fig. 3c).

Next, we focussed on the unique aspects of the α-α′-α″-type or to the β-β′-type interactions. Among the contacts between α-helices, the salt bridge between Asp 307 and Arg 311 is unique to the α-α′-α″-type interaction, and disrupting this contact by changing Arg311 to alanine (R311A) should specifically affect the α-α′-α″-type interaction. Similarly, changing Leu 304 to phenylalanine in combination with Phe 303 to Ala (F303A-L304F) should sterically hinder the β-β′-type interaction. The side chain of the phenylalanine 304 would point away to the hydrophobic core of α-α′-α″-type interaction, but would obstruct the hydrophobic contact of β-β′-type interaction, thus the disruption would become β-β′-type specific (Fig. 3a). Sucrose sedimentation analysis of these two mutants showed that both of them were distributed in fractions corresponding to small particles or aberrant assemblies (Fig. 3b). Observation by EM revealed that R311A and F303A-L304F formed small spherical particles, with mean diameters of 28.8 and 22.5 nm, respectively (Fig. 3c, R311A, F303A-L304F). Mutations designed to disrupt both type of interactions were also constructed: D307A-R311A diminished a salt-bridge interaction, and L304W disrupted hydrophobic contacts by a bulky side chain. EM revealed that D307A-R311A and L304W formed small spherical particles, with mean diameters of 24.7 nm (D307A-R311A) and 33.5 nm (L304W) (Fig. 3c, D307A-R311A, L304W). Sucrose gradient sedimentation analysis showed that the majority of these VP1 mutants was found in fractions 3–8 (Fig. 3b, D307A-R311A, L304W), which is consistent with the results of EM observations.

The spherical particles of about 20 nm in diameter likely correspond to a $T=1$ tiny particle. Analysis using cryoelectron tomography showed that the C-terminal region of BKV VP1, which assembles into $T=1$ particles, adopts a triple α-helical bundle structure, reminiscent of the α-α′-α″-type contact, in which all of the helices are in the identical conformation (*20*). Therefore, restricting the conformational flexibility of *Region I* could lead to $T=1$-like particle formation. Our results showed that *Region I* VP1 point mutants formed protein aggregates (L305P and L308P) or small particles (R311A, F303A-L304F, D307A-R311A and L304W). We hypothesize that VP1 pentamers initially form α-α′-α″-like contacts, then each VP1 pentamer adopts the proper α-helical conformation (α, α′, α″, β and β′ conformation) as well as loop structure (γ conformation) for assembling into an icosahedral capsid with a $T=7d$ lattice. This would account for the formation of small, $T=1$-like particles by *Region I* VP1 point mutants. For example, the F303A-L304F mutant, designed to block the β-β′ contact, assembled into $T=1$-like particles, perhaps due to inability to properly switch the conformation for generating $T=7d$ icosahedral symmetry owing to blockage to proceed to the β-β′-type interaction. The R311A mutant formed a $T=1$-like tiny particles possibly because the mutation weakened the α-α′-α″ interaction thereby unable to stabilize the structural switch. Similarly, in mutants both type of interactions, α-α′-α″- and β-β′-types, were disrupted, such as in VP1s of D307A-R311A, and L304W, the structural switch would be more severely interfered. However, the size of particles assembled by such mutants were somewhat varied, from about 20–30 nm in diameter, and may not fit to the typical $T=1$ particles. Detailed analysis on the mutant particles, counting number of pentamers constitute the particles, and structural examination of the C-terminal conformation, would provide better basis on examination of our hypothesis and will be a next study.

Substitution of SV40 Region I with MPV or AGMPV Region I—The analysis on point-mutants revealed that *Region I* holds important function on controlling inter-pentamer interaction for generating proper icosahedral symmetry. To determine whether *Region I* is functionally independent, we substituted *Region I* of SV40 with that of murine polyomavirus (MPV) or African green monkey polyomavirus (AGMPV). The amino acid resides of *Region I* of MPV and AGMPV are quite distinct; only one leucine (Leu 304) among 12 residues is conserved. The structure of MPV *Region I* has been resolved, and is distinct from that of SV40 (*21*). The α-helical bundles are stacked together only via hydrophobic contacts, without the salt-bridges that are seen in SV40. Chimeric SV40 VP1s harboring *Region I* of MPV or AGMPV (SV-MVP and SV-AGMVP, respectively) were expressed in insect

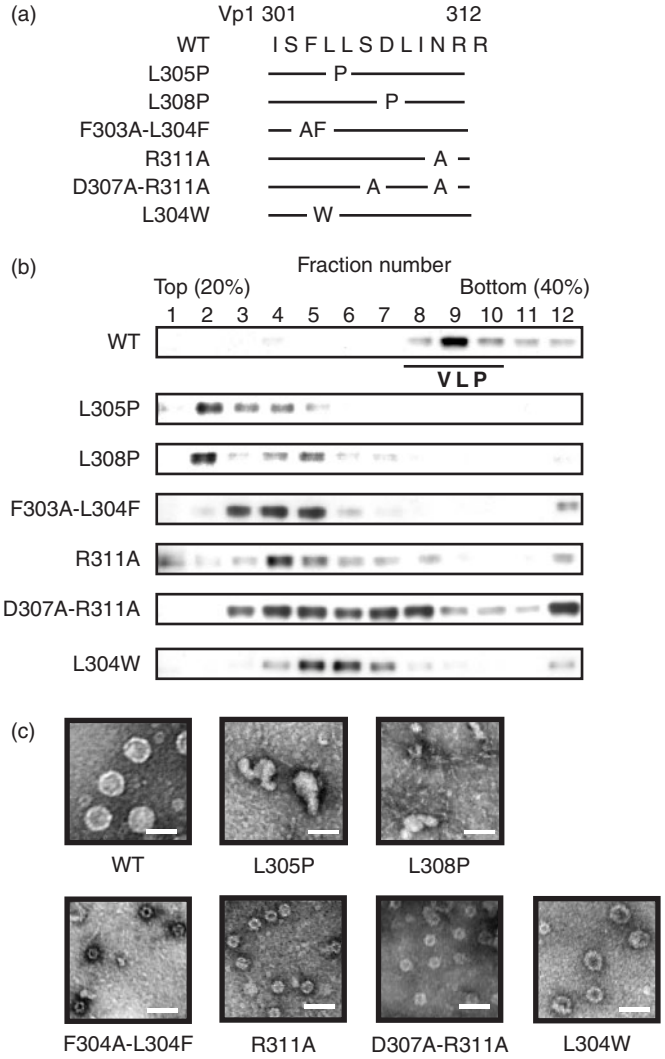

Fig. 3. **Assembly of C-terminal α-helical region point mutants of VP1 expressed in Sf-9 cells.** (**a**) Schematic representation of VP1 C-terminal *Region I* point mutants. Amino acid residues are represented by one-letter code. (**b**) Sucrose gradient sedimentation analysis. Cell lysates containing the indicated VP1 point mutants were analysed as described in Fig. 2c. (**c**) Electron micrographs of VP1 point mutants were purified and visualized as described in Fig. 2b. Scale bar is 100 nm.

cells and analysed for their ability to form particles. Sucrose gradient analysis showed that SV-MPV was present in fractions 5–8. The SV-AGMPV chimera was present in fractions 3–9. These results indicate that they formed particles or structures smaller than VLPs. EM observation showed that the mean diameter of SV-MPV or SV-AGMPV particles was 30.0 and 28.3 nm, respectively (Fig. 4c). These results, showing that *Region I* from another virus cannot functional substitute for SV40 *Region I*, suggested that *Region I* is not functionally separable. Our hypothesis would predict that upon forming α-α′-α″-like contacts, VP1 *Region I* must adopt a proper conformational switch, which would likely influenced by structural motifs adjacent to *Region I*. In the absence of such structural motifs, as in the case of chimeric VP1, SV-MPV and SV-AGMPV, structural switch may not proceed efficiently. Although the structural study showed that interactions in *Region I* does not have additional contacts with other VP1 regions (*1*, 2), *Region I* could transiently interact with other regions of the interacting VP1 with which functions as guiding proper assembly of the VP1 pentamer. *Region I* of MPV or AGMPV could also functions as combination with other regions of the interacting VP1.

Our analysis on the SV40 VP1-C-terminal region can be divided into two parts: (i) Upon progressive deletion of the SV40 C-terminal arm and examined their ability to form assemblies we found that the C-terminal regions are collectively important for proper VP1-self-assembly. (ii) Point-mutational approach on the very proximal domain of C-terminal arm, *Region I*, revealed that *Region I* is important for directing proper self-assembly of VP1 pentamer to form a full capsid. The two conclusions fit nicely with the existing structural model of the SV40 capsid and also provide a new insight. *Regions II*, *III* and *IV* directly contact and interdigitate

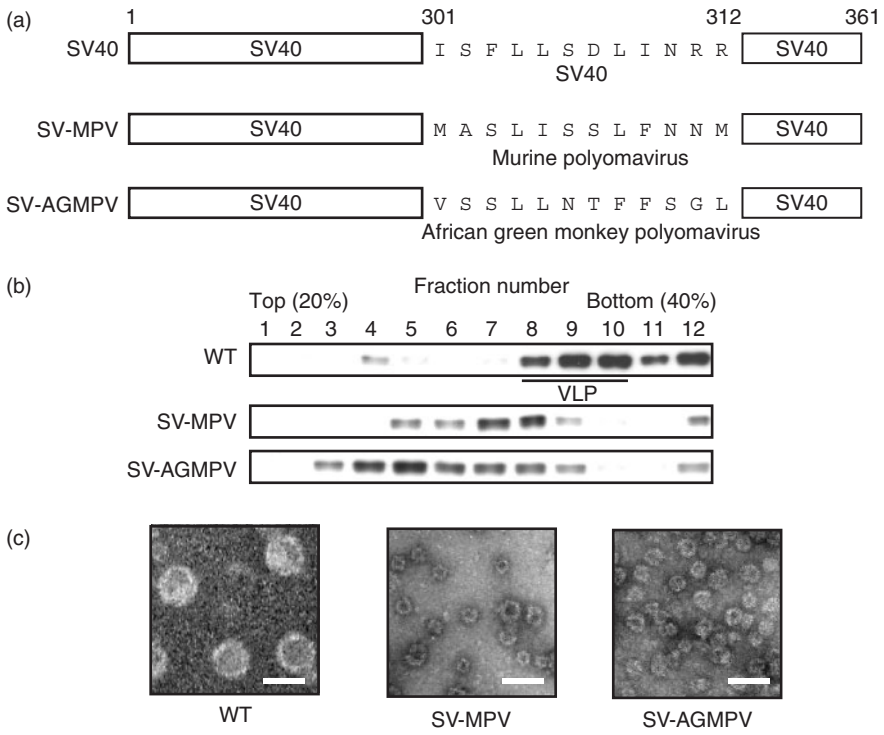

Fig. 4. **Assembly of VP1 carboxyl-terminal α-helical region chimeras expressed in Sf-9 cells.** (**a**) Schematic representation of VP1 C-terminal α-helical region chimeras. Amino acid residues are represented by one-letter code. (**b**) Sucrose gradient sedimentation analysis of α-helical region VP1 chimeras containing *Region I* from Murine polyomavirus (SV-MPV) and African green monkey polyomavirus (SV-AGMPV). Cell lysates containing the indicated VP1 chimeras were analysed as described in Fig. 2c. (**c**) Electron micrographs of VP1 chimeras purified and visualized as described in Fig. 2b. Scale bar is 100 nm.

with the N-terminus of interacting VP1. Not surprisingly, progressive deletion of these regions led to progressive loss of ability of the VP1 to self-assemble and form a capsid. In contrast, *Region I* contacts only with the incoming C-terminal arm from the interacting VP1. The structural model suggests that *Region I* adopts highly variable conformation depending on the position of pentamer in the icosahedral lattice. Perhaps such structural mobility could be a key to control proper inter-pentamer interaction to generate full capsid assemblies. Indeed, our point-mutational approach revealed that mutant VP1 aimed to be restricted in certain conformation self-assembled to particles but much smaller than the full capsid, indicating that *Region I* is not essential for self-assembly of VP1 pentamer, but rather important for guiding and adjusting the inter-pentamer interaction to form full capsid formation. Our results also indicate that by controlling the conformational switch in *Region I* it is possible to alter the symmetry of capsid implying potential flexibility of viral capsid proteins to self-assemble. Further understanding of the basis of viral assembly would pave a way to potential use of viral capsid proteins as a building block for a novel nanostructure of industrial or pharmaceutical use.

This work was supported by a Grant-in-Aid for Scientific Research and of the 21st Century COE program from the Ministry of Education, Culture, Sports, Science, and Technology in Japan, and a grant for research and development projects in Cooperation with Academic Institutions from the New Energy and Industrial Technology Development Organization (NEDO). We are grateful to Dr Osamu Nureki and Dr Kosuke Kataoka for helpful discussion.

REFERENCES

1. Liddington, R.C., Yan, Y., Moulai, J., Sahli, R., Benjamin, T.L., and Harrison, S.C. (1991) Structure of simian virus 40 at 3.8-A resolution. *Nature* **354**, 278–284
2. Stehle, T., Gamblin, S.J., Yan, Y., and Harrison, S.C. (1996) The structure of simian virus 40 refined at 3.1 A resolution. *Structure* **4**, 165–182
3. Garcea, R.L., Salunke, D.M., and Caspar, D.L. (1987) Site-directed mutation affecting polyomavirus capsid self-assembly *in vitro*. *Nature* **329**, 86–87
4. Schwartz, R., Garcea, R.L., and Berger, B. (2000) "Local rules" theory applied to polyomavirus polymorphic capsid assemblies. *Virology* **268**, 461–470
5. Ishizu, K.I., Watanabe, H., Han, S.I., Kanesashi, S.N., Hoque, M., Yajima, H., Kataoka, K., and Handa, H. (2001) Roles of disulfide linkage and calcium ion-mediated interactions in assembly and disassembly of virus-like particles composed of simian virus 40 VP1 capsid protein. *J. Virol.* **75**, 61–72
6. Sandalon, Z., Dalyot-Herman, N., Oppenheim, A.B., and Oppenheim, A. (1997) *In vitro* assembly of SV40 virions and pseudovirions: vector development for gene therapy. *Hum. Gene Ther.* **8**, 843–849
7. Chang, D., Fung, C.Y., Ou, W.C., Chao, P.C., Li, S.Y., Wang, M., Huang, Y.L., Tzeng, T.Y., and Tsai, R.T. (1997) Self-assembly of the JC virus major capsid protein, VP1, expressed in insect cells. *J. Gen. Virol.* **78**, 1435–1439

8. Ou, W.C., Wang, M., Fung, C.Y., Tsai, R.T., Chao, P.C., Hseu, T.H., and Chang, D. (1999) The major capsid protein, VP1, of human JC virus expressed in Escherichia coli is able to self-assemble into a capsid-like particle and deliver exogenous DNA into human kidney cells. *J. Gen. Virol.* **80**, 39–46
9. Li, T.C., Takeda, N., Kato, K., Nilsson, J., Xing, L., Haag, L., Cheng, R.H., and Miyamura, T. (2003) Characterization of self-assembled virus-like particles of human polyomavirus BK generated by recombinant baculoviruses. *Virology* **20**, 115–124
10. Touze, A., Bousarghin, L., Ster, C., Combita, A.L., Roingeard, P., and Coursaget, P. (2001) Gene transfer using human polyomavirus BK virus-like particles expressed in insect cells. *J. Gen. Virol.* **82**, 3005–3009
11. Forstova, J., Krauzewicz, N., Wallace, S., Street, A.J., Dilworth, S.M., Beard, S., and Griffin, BE. (1993) Cooperation of structural proteins during late events in the life cycle of polyomavirus. *J. Virol.* **67**, 1405–1413
12. Montross, L., Watkins, S., Moreland, R.B., Mamon, H., Caspar, D.L., and Garcea, R.L. (1991) Nuclear assembly of polyomavirus capsids in insect cells expressing the major capsid protein VP1. *J. Virol.* **65**, 4991–4998
13. An, K., Smiley, S.A., Gillock, E.T., Reeves, W.M., and Consigli, R.A. (1999) Avian polyomavirus major capsid protein VP1 interacts with the minor capsid proteins and is transported into the cell nucleus but does not assemble into capsid-like particles when expressed in the baculovirus system. *Virus Res.* **64**, 173–185
14. Rodgers, R.E., Chang, D., Cai, X., and Consigli, R.A. (1994) Purification of recombinant budgerigar fledgling disease virus VP1 capsid protein and its ability for *in vitro* capsid assembly. *J. Virol.* **68**, 3386–3390
15. Wrobel, B., Yosef, Y., Oppenheim, A.B., and Oppenheim, A. (2000) Production and purification of SV40 major capsid protein (VP1) in Escherichia coli strains deficient for the GroELS chaperone machine. *J. Biotechnol.* **84**, 285–289
16. Salunke, D.M., Caspar, D.L., and Garcea, R.L. (1986) Self-assembly of purified polyomavirus capsid protein VP1. *Cell* **46**, 895–904
17. Kosukegawa, A., Arisaka, F., Takayama, M., Yauima, H., Kaidow, A., and Handa, H. (1996) Purification and characterization of virus-like particles and pentamers produced by the expression of SV40 capsid proteins in insect cells. *Biochim. Biophys. Acta* **1290**, 37–45
18. Kanesashi, S.N., Ishizu, K.I., Kawano, M.A., Han, S.I., Tomita, S., Watanabe, H., Kataoka, K., and Handa, H. (2003) Simian virus 40 VP1 capsid protein forms polymorphic assemblies *in vitro*. *J. Gen. Virol.* **84**, 1899–1905
19. Kawano, M.A., Inoue, T., Tsukamoto, H., Takaya, T., Enomoto, T., Takahashi, R.U., Yokoyama, N., Yamamoto, N., Nakanishi, A., Imai, T., Wada, T., Kataoka, K., and Handa, H. (2006) The VP2/VP3 minor capsid protein of simian virus 40 promotes the *in vitro* assembly of the major capsid protein VP1 into particles. *J. Biol. Chem.* **281**, 10164–10173
20. Nilsson, J., Miyazaki, N., Xing, L., Wu, B., Hammar, L., Li, T.C., Takeda, N., Miyamura, T., and Cheng, R.H. (2005) Structure and assembly of a $T=1$ virus-like particle in BK polyomavirus. *J. Virol.* **79**, 5337–5345
21. Stehle, T. and Harrison, S.C. (1996) Crystal structures of murine polyomavirus in complex with straight-chain and branched-chain sialyloligosaccharide receptor fragments. *Structure* **4**, 183–194
22. Reddy, V.S., Natarajan, P., Okerberg, B., Li, K., Damodaran, K.V., Morton, R.T., Brooks, C.L. 3rd, and Johnson, J.E. (2001) Virus Particle Explorer (VIPER), a website for virus capsid structures and their computational analyses. *J. Virol.* **75**, 11943–11947